

Article

Simultaneous Detection of Serotonin and 17 β -Estradiol Using rGO/SPCE Modified with Cu(II) Complex: A Novel Approach for PMDD Diagnosis

Claudia Núñez ^{1,*} , Ronald Nelson ¹ , Gerald Tabilo ¹, Paulina Pefaur ¹, Rodrigo Castillo ¹ 
and Alifhers Mestra ^{1,2} 

¹ Departamento de Química, Facultad de Ciencias, Universidad Católica del Norte, Avda. Angamos 0610, Antofagasta 1270709, Chile; rnelson@ucn.cl (R.N.); gerald.tabilo@alumnos.ucn.cl (G.T.); paulina.pefaur@alumnos.ucn.cl (P.P.); rocastillo@ucn.cl (R.C.); alifhers.mestra@ce.ucn.cl (A.M.)

² Centro Lithium I+D+i, Universidad Católica del Norte, Avenida Angamos 0610, Antofagasta 1270709, Chile

* Correspondence: cnunez@ucn.cl

Abstract: Approximately 4% of women of reproductive age are estimated to suffer from premenstrual dysphoric disorder (PMDD), a condition likely underdiagnosed due to various biases, suggesting that actual prevalence may be higher. Addressing this, a novel electrochemical sensor was developed using a screen-printed electrode of reduced graphene oxide modified with a Cu(II) triazole complex, Cu(L^{NO₂})₂/rGO/SPCE. This sensor aims to determine levels of serotonin and 17 β -estradiol rapidly, and simultaneously, key analytes implicated in PMDD. The method demonstrated high sensitivity for both analytes, achieving sensitivity levels of 0.064 $\mu\text{A}/\mu\text{mol L}^{-1}$ for serotonin and 0.055 $\mu\text{A}/\mu\text{mol L}^{-1}$ for 17 β -estradiol, with a linear detection range of 2 to 42 $\mu\text{mol L}^{-1}$. Detection limits were 42 nmol L⁻¹ for serotonin and 53 nmol L⁻¹ for estrogen. The sensor also exhibited high stability and selectivity against common interferences found in biological fluids. It was successfully used to measure serotonin and 17 β -estradiol in human serum and urine, with recovery percentages within the expected ranges. This demonstrates that the sensor proposed in this work holds significant potential to contribute not only to the accurate diagnosis of such disorders but also to their treatment. We hope that this research will pave the way for the development of devices that have a positive impact on the quality of life of women suffering from multisystem diseases caused by hormonal malfunctions.

Keywords: PMDD; Serotonin; 17 β -estradiol; Cu(II) triazole complexes; rGO



Citation: Núñez, C.; Nelson, R.; Tabilo, G.; Pefaur, P.; Castillo, R.; Mestra, A. Simultaneous Detection of Serotonin and 17 β -Estradiol Using rGO/SPCE Modified with Cu(II) Complex: A Novel Approach for PMDD Diagnosis. *Chemosensors* **2024**, *12*, 164. <https://doi.org/10.3390/chemosensors12080164>

Received: 8 July 2024

Revised: 4 August 2024

Accepted: 12 August 2024

Published: 17 August 2024



Copyright: © 2024 by the authors. Licensee MDPI, Basel, Switzerland. This article is an open access article distributed under the terms and conditions of the Creative Commons Attribution (CC BY) license (<https://creativecommons.org/licenses/by/4.0/>).

1. Introduction

Premenstrual disorders consist of a set of somatic and psychiatric symptoms that occur in the luteal phase of the menstrual cycle [1]. The International Society for the Study of Premenstrual Disorders (ISPM) classifies premenstrual symptoms into 3 groups: (i) women who have presented occasional psychiatric and somatic symptoms during the luteal phase; (ii) women who present Premenstrual Syndrome (PMS) where the symptoms can affect daily life; and (iii) Premenstrual Dysphoric Disorder (PMDD), where severe and disabling symptoms occur, significantly affecting quality of life and female productivity [1–3]. It has been reported that 80% of women of reproductive age have experienced minor symptoms associated with PMS, 12% have been diagnosed with PMS and 4% suffer from PMDD, the latter comes with much uncertainty because the symptoms are similar to those of bipolar affective disorder (BAD), confusing its diagnosis [2–4]. PMS is associated with somatic symptoms such as headaches, muscle pain, a feeling of fullness, weight gain, change in appetite, lack of energy, insomnia or hypersomnia, breast tenderness, pelvic pain, and abdominal distention [5]. The diagnostic criteria for PMDD, as defined by the American Psychiatric Association (APA) in the DSM-V, include somatic symptoms described and

psychiatric symptoms such as anger outbursts, anxiety, mental confusion, depression, irritability, social withdrawal, difficulty concentrating, and subjective feeling of being overwhelmed [5].

The affective symptoms related to these disorders represent a considerable and worrying burden, as they can make women particularly susceptible to suicidal tendencies, including ideation, planning, or even attempts. In this context, several studies have successfully associated suicide attempts in women with specific phases of their menstrual cycle and with levels of steroid hormones such as estrogen and progesterone [6–12]. Papadopoulou et al. [9] found that 59% of suicide attempts by women occurred during the last four days of the luteal phase and the first four days of menstruation. On the other hand, Leenaraars et al. [8] carried out a study to evaluate the influence of the menstrual cycle on suicide. They performed autopsies on 56 women who had completed suicides and compared the findings with 44 women who died from other causes. The results indicated that 25% of the women who had committed suicide were menstruating at the time of death, compared to 4.5% of the control group. This led to the statistical conclusion that there might be an association between menstruation and suicide in women.

The etiology of PMDD is still an area of active research. Among the potential causes under investigation are genetic factors and stress-related mechanisms [13]. Identified mechanisms include involvement of the following: steroid hormones such as progesterone, estradiol [14], and cortisol [15]; neurosteroids like allopregnanolone [16]; and neurotransmitters including GABA_A receptors and serotonin [17]. The progesterone metabolite involved in PMDD is allopregnanolone (AP α). This neuroactive steroid acts as a positive allosteric modulator of the GABA_A receptor, exhibiting anxiolytic, anesthetic, and sedative properties. On the other hand, estradiol exerts potent effects on multiple neurotransmitter systems, playing a crucial role in regulating mood, cognition, sleep, eating, and various other behavioral aspects. Research has established that ovarian steroids alter the expression of the 5-HT_{2A} receptor and the serotonin transporter (SERT). Clinically, women with PMDD exhibit specific abnormalities in serotonin (5-HT) levels, particularly evident in the late luteal phase when estrogen levels have decreased. These abnormalities manifest as low mood, cravings for specific foods, and poor cognitive performance [1,6,18,19].

Although previous studies have linked PMS or PMDD with suicidal tendencies and have identified the involved analytes, research on this condition remains limited. Of the few studies conducted, most focus on the psychiatric aspect, often overlooking physiological investigations in both diagnosis and treatment. This limitation can be attributed to the use of analytical techniques such as liquid chromatography, fluorescence and gas chromatography, as well as enzyme-linked immunoassay techniques for detecting estrogen, progesterone, and serotonin [20–27]. Despite their excellent analytical capabilities, these methods pose challenges, such as cost and analysis time, for conducting studies that accurately profile the variation of these analytes in the menstrual cycle. In this field, electrochemical sensors are in a unique position to allow the miniaturization of a clinical laboratory.

Currently, no electrochemical device capable of simultaneously determining estradiol and serotonin with a focus on PMDD detection and control has been developed. Regarding serotonin, several analytical methodologies have been reported for its detection in human serum and urine samples using electrodes modified with various materials. Yilmaz et al. [28] reported ultrasensitive electrochemical sensors for the simultaneous determination of dopamine and serotonin, using a SPCE modified with TiO₂NP, achieving detection limits of 2.47 nmol L⁻¹ for serotonin. In contrast, Gholivand et al. [29] developed a method for the simultaneous determination of dopamine, serotonin, and tryptophan using a carbon paste electrode modified with ZrO₂-CuO co-doped with CeO₂, reaching detection limits of 3.49 nmol L⁻¹. Both methodologies exhibit excellent detection limits; however, they do not include estradiol in their determinations. Regarding estradiol determination, Honeychurch et al. [30] developed a methodology using SPCE modified with rGO-AuNPs/CNT, reporting a detection limit of 3 nmol L⁻¹. However, this methodology was used for water samples. Conversely, Lingling et al. [31] reported a method applied to human serum

samples. They modified a glassy carbon electrode with a wrinkled mesoporous carbon nanomaterial, obtaining a detection limit of 8.3 nmol L^{-1} .

In this context, with the aim of developing a portable, fast, and direct analytical method for the simultaneous determination of serotonin and estrogen, we fabricated a sensor based on the modification of a reduced graphene oxide screen printed electrode (rGO/SPCE) with a Cu(II) triazole complex substituted with nitro groups on the phenyl ring (see Figure 1). This complex was synthesized by Nelson et al., who studied its capacity for hydrogen peroxide and sulfite detection [32,33]. In these studies, the authors reported the excellent electrocatalytic properties of $\text{Cu}(\text{L}^{\text{NO}_2})_2$ complex, attributing them to the resonance effect between the triazole and phenyl rings substituted with electron withdrawing groups. In addition, the nitro group in the phenyl ring enhances the reduction capacity of the complex due to its electron-accepting nature, thereby improving the electroactive capacity in the oxidation of species.

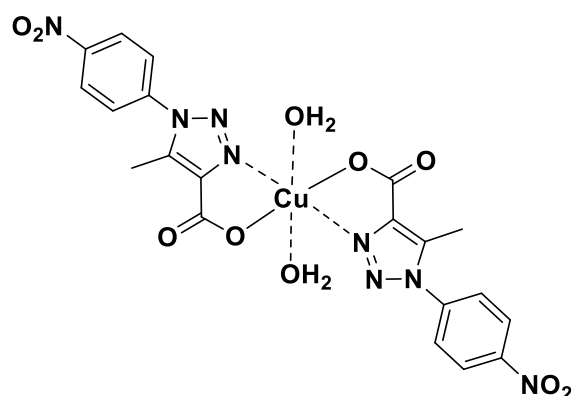


Figure 1. Chemical structure of copper(II) complexes $\text{Cu}(\text{L}^{\text{NO}_2})_2$ [32].

2. Materials and Methods

2.1. Reagents

Serotonin (CAS 50-67-9), Estrogen 17β -estradiol (CAS 50-28-2), Ethanol (CAS 64-17-5), dihydrogen phosphate (KH_2PO_4) (CAS 7778-77-0), dipotassium hydrogen phosphate (K_2HPO_4) (CAS 7758-11-4), dopamine (CAS 62-31-7), uric acid (CAS 69-93-2), ascorbic acid (CAS 50-81-7), potassium chloride, potassium hexacyanoferrate (II) trihydrate, potassium hexacyanoferrate (II) trihydrate, and human serum (P2918) were purchased from Sigma-Aldrich. Synthetic human urine (BR-397) was purchased from Bio-Rad Laboratories. Screen-printed reduced graphene oxide (refs.110-RGPHOX) was purchased from DropSens (Madrid, Spain). Deionized water for sample preparation, dilution of reagents, and rinsing purposes was obtained from the laboratory water system Adrona CB 1901 (resistivity: $18.2 \text{ M}\Omega$).

2.2. Apparatus

SEM images were obtained using a Hitachi FE-SEM SU5000 (Hitachinaka, Japan) with XFlash 6I30, Bruker detector. Raman spectra were collected using a Confocal Raman Microscope (Jasco, NRS-4500, Easton, MD, USA), equipped with an air-cooled Peltier CCD detector, and employing a 785 nm wavelength laser. The scanned range was from 50 to 4000 cm^{-1} , at a data interval of 1 cm^{-1} , collecting three accumulations of 90 s each, and using a laser power of 0.3 mW to avoid damage to the samples. Electrochemical measurements were carried out on a Potentiostat/Galvanostat Origaflex OGF05A with an impedance module OGFEIS.

2.3. Fabrication of $\text{Cu}(\text{L}^{\text{NO}_2})_2/\text{rGO}/\text{SPCE}$

The preparation of the Cu(II) triazole complex was carried out as described by Nelson et al. [32]. $\text{Cu}(\text{L}^{\text{NO}_2})_2$ was diluted to 1 mg mL^{-1} in DMF reagent and sonicated for 30 min.

This solution was homogenized by stirring, and then 2 μL was coated over the working electrode's surface and dried at a temperature of 60 $^{\circ}\text{C}$ for 10 min. This procedure was repeated successively until reaching a total volume of 10 μL of Cu(II) triazole complex (1 mg mL^{-1}).

2.4. Electrochemical Measurements

The electrochemical cell was composed of a modified $\text{Cu}(\text{L}^{\text{NO}_2})_2/\text{rGO}$ screen-printed electrode and supporting electrolyte with a 40%/60% (*v/v*) mixture of ethanol and phosphate buffer solution. PB was prepared by mixing K_2HPO_4 and KH_2PO_4 solutions at 0.1 M and pH 7.0, and the pH was adjusted with 4.0 mol L^{-1} of sodium hydroxide solution. For analyte measurement, a mixture of 10 mmol L^{-1} serotonin and 10 mmol L^{-1} 17 β -estradiol stock solution was prepared in ethanol. A solution of 1 mmol L^{-1} serotonin and 1 mmol L^{-1} 17 β -estradiol was prepared daily from this stock solution and diluted in a mixture of 40% ethanol and 60% 0.1 mol L^{-1} phosphate buffer solution. Linear sweep voltammetry (LSV) was carried out over a potential range of 0.0 to 1.0 V at a scan rate of 50 mV s^{-1} . Cyclic voltammetry (CV) was performed from -800 to 800 mV with a sweep speed of 50 mV s^{-1} . Impedance measurements were performed with frequency from 0.1 to 400 kHz, pulse amplitude of 10 mV, and open circuit using $\text{KCl } 0.1 \text{ mol L}^{-1}/[\text{Fe}(\text{CN})_6]^{3-/4-}$.

3. Results

3.1. Morphological Characterization of $\text{Cu}(\text{L}^{\text{NO}_2})_2/\text{rGO}/\text{SPCE}$

Morphologically, characterization by field emission scanning electron microscopy (FE-SEM) and elemental mapping of SPCE, rGO/SPCE, and $\text{Cu}(\text{L}^{\text{NO}_2})_2/\text{rGO}/\text{SPCE}$ were performed, as shown in Figure 2a–c. SPCE and rGO/SPCE exhibited typical morphology of commercial electrodes (Figure 2a,b). Elemental mapping corroborated the presence of Cu on the surface of the modified rGO/SPCE and revealed a smooth film, indicating that $\text{Cu}(\text{L}^{\text{NO}_2})_2$ covered the electrode surface with a homogeneous film (Figure 2c). The Raman spectra of pure SPCE, rGO/SPCE, $\text{Cu}(\text{L}^{\text{NO}_2})_2/\text{rGO}/\text{SPCE}$, and $\text{Cu}(\text{L}^{\text{NO}_2})_2$ pure complexes were analyzed and depicted in Figure 3. The G and D bands, corresponding to the in-plane stretching vibrations of the sp^2 carbons and the ring breathing mode from the sp^2 carbons ring, respectively, were throughout the electrode preparation process. Furthermore, pure SPCE exhibited the highest intensity of the characteristic G and D bands, indicating the successful dispersion of the complex and rGO on the electrode by comparing the Raman spectra. Additional evidence is obtained by examining the peak shapes, which generally broaden as the bare electrode is prepared with rGO and subsequently with the complex. The latest spectra show the widest peaks, as these signals include the Raman modes present in the same region as the complex.

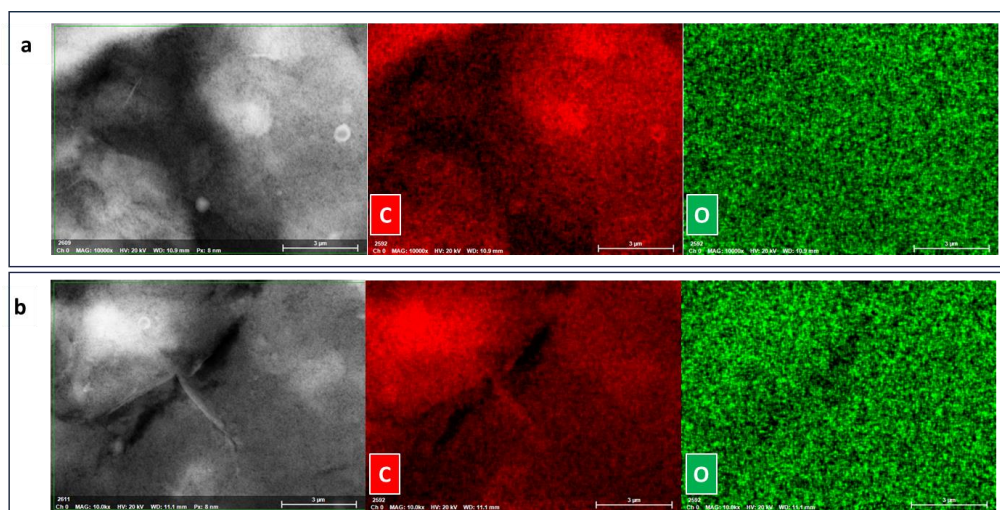


Figure 2. Cont.

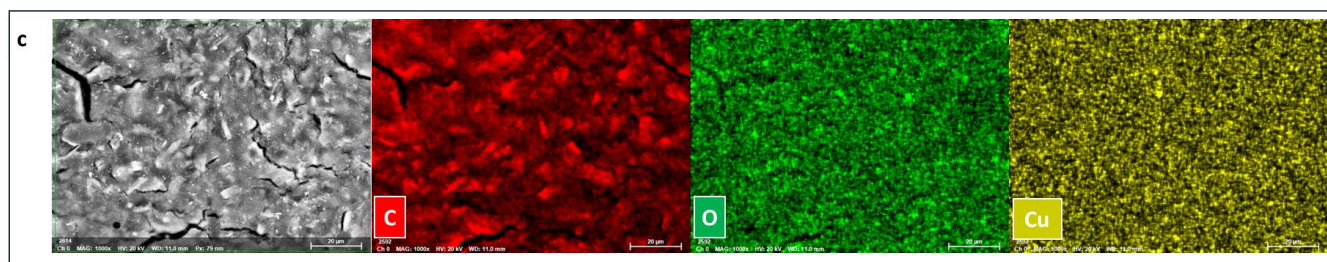


Figure 2. SEM and EDS element mapping images of (a) SPCE, (b) rGO/SPCE, and (c) $\text{Cu}(\text{L}^{\text{NO}_2})_2/\text{rGO}/\text{SPCE}$. See EDS spectra in supporting materials (Figure S1).

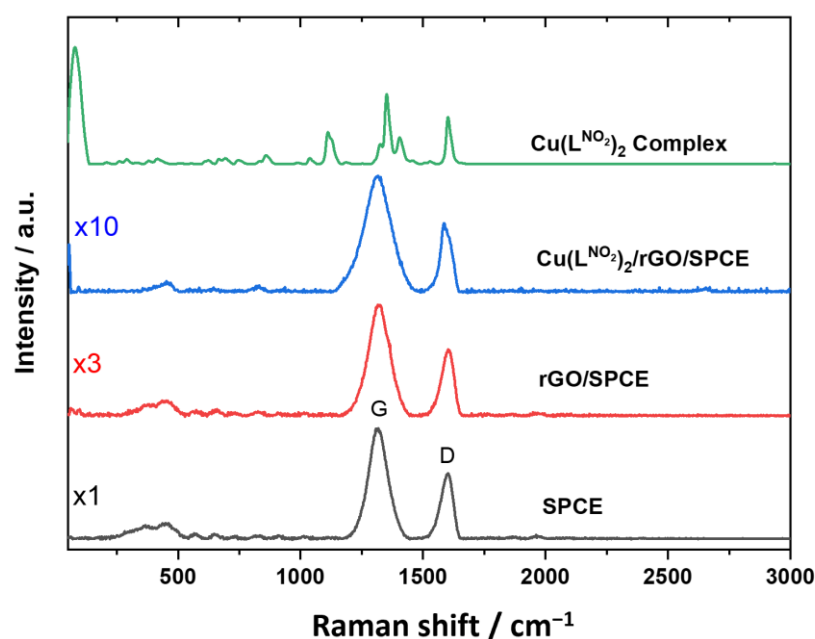


Figure 3. Raman spectra of a SPCE, rGO/SPCE, $\text{Cu}(\text{L}^{\text{NO}_2})_2/\text{rGO}/\text{SPCE}$, and $\text{Cu}(\text{L}^{\text{NO}_2})_2$ pure complex.

3.2. Electrochemical Characterization of $\text{Cu}(\text{L}^{\text{NO}_2})_2/\text{rGO}/\text{SPCE}$

The electrochemical performance of unmodified SPCE and modified rGO/SPCE and $\text{Cu}(\text{L}^{\text{NO}_2})_2/\text{rGO}/\text{SPCE}$ was studied using cyclic voltammetry in the presence of $5 \text{ mmol L}^{-1} [\text{Fe}(\text{CN})_6]^{3-/4-}$ in 0.1 M KCl . Electrochemical impedance spectroscopy (EIS) was utilized to evaluate the interfacial properties of the $\text{Cu}(\text{L}^{\text{NO}_2})_2$ modified electrode. Cyclic voltammograms are shown in Figure 4a. A well-defined redox peak appears at SPCE and rGO/SPCE; however, when the electrode was modified with $\text{Cu}(\text{L}^{\text{NO}_2})_2$, the reversibility of the model system $[\text{Fe}(\text{CN})_6]^{3-/4-}$ decreased, shifting the signals to less positive potentials. The current intensity of the redox couple peaks increased when $\text{Cu}(\text{L}^{\text{NO}_2})_2$ was deposited on the electrode surface, demonstrating that its conductive characteristics facilitate electron transfer. The Nyquist diagram and equivalent circuit model used for the three electrodes are represented in Figure 4b, where R_s indicates the resistance to the electrolyte, R_{ct} is the resistance to charge transfer and W_o is the Warburg resistance. The results obtained showed that the R_s for the rGO electrode was 2.24Ω which is lower than that for $\text{Cu}(\text{L}^{\text{NO}_2})_2/\text{rGO}$ and SPCE, with resistance values 2.75 and 2.31Ω , respectively, indicating that rGO improves the electrode wettability. However, the $\text{Cu}(\text{L}^{\text{NO}_2})_2$ addition increased the resistance of the electrolyte probably due to the polar properties of 4-nitrophenyl-1,2,3-triazole groups in the complex structure (see Table S2 in supporting materials). On the other hand, the charge transfer resistance (R_{ct}) was determined, showing a lowest semicircle in the Nyquist diagram for $\text{Cu}(\text{L}^{\text{NO}_2})_2/\text{rGO}/\text{SPCE}$ (see inset of Figure 4b). The determined resistance values were 767.40 , 836.70 , and 869.40Ω for $\text{Cu}(\text{L}^{\text{NO}_2})_2/\text{rGO}/\text{SPCE}$, rGO/SPCE, and SPCE, respectively, demonstrating that the addition of the $\text{Cu}(\text{L}^{\text{NO}_2})_2$ complex on the

rGO electrode surface improves the charge transfer attributable to the conjugated character of $\text{Cu}(\text{L}^{\text{NO}_2})_2$ structure. This property allows greater charge transfer [32]. Finally, the electron-withdrawing properties of the $-\text{NO}_2$ group caused a shift of the copper redox couple towards more cathodic potentials, allowing a rapid charge transfer and a higher electron flow at a lower energy cost than electrodes. This can also be demonstrated with the Warburg resistance (W_o), which is related to the diffusion processes at the electrode/electrolyte interface. The values obtained for $\text{Cu}(\text{L}^{\text{NO}_2})_2/\text{rGO}/\text{SPCE}/$ was 5.34Ω , while that for the electrode of rGO/SPCE was 6.57Ω and SPCE was 10.34Ω , indicating that the complex improves electronic transfer processes and shows less dependence on controlled processes by diffusion and mass transport.

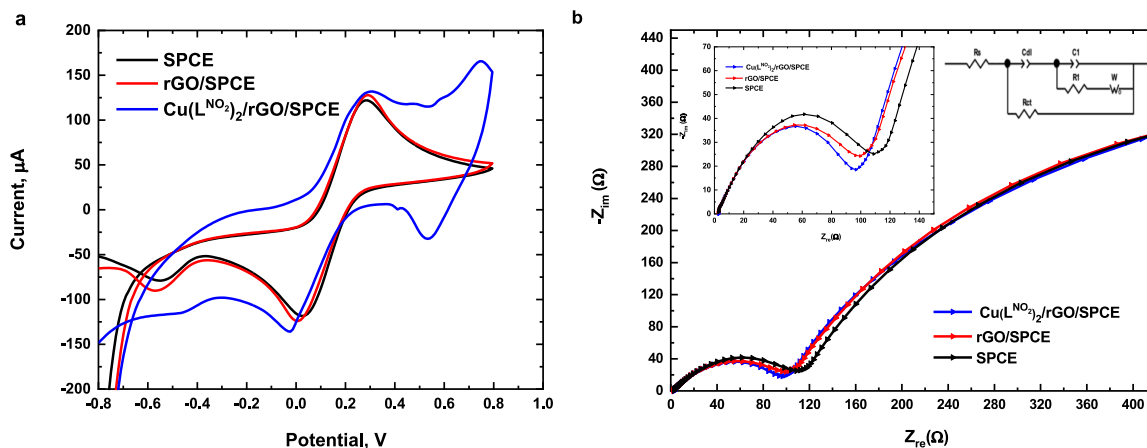


Figure 4. (a) Cyclic voltammograms (b) Nyquist plot of SPCE, rGO/SPCE, and $\text{Cu}(\text{L}^{\text{NO}_2})_2/\text{rGO}/\text{SPCE}$ in $5 \text{ mmol L}^{-1} [\text{Fe}(\text{CN})_6]^{3-/4-}$ $0.1 \text{ mol L}^{-1} \text{ KCl}$.

3.3. Electrochemical Performance of $\text{Cu}(\text{L}^{\text{NO}_2})_2/\text{rGO}/\text{SPCE}$

Initially, the electrochemical oxidation of serotonin and 17β -estradiol were studied by linear sweep voltammetry (LSV) on four different electrochemical platforms: (i) SPCE; (ii) nAu/SPCE; (iii) nPEDOT/SPCE; and (iv) rGO/SPCE, all modified with 1 mg mL^{-1} of $\text{Cu}(\text{L}^{\text{NO}_2})_2$ (Figure 5a,b). The analytes signals were monitored in a potential range from 0.0 to 1.0 V and at a scan rate of 50 mV/s . The results showed that when the $\text{Cu}(\text{L}^{\text{NO}_2})_2$ complex was added to the SPCE surface, a very small signal current was observed for 17β -estradiol ($0.31 \mu\text{A}$). Similarly, for nAu/SPCE, the signal current intensity was low for both analytes ($0.38 \mu\text{A}$ for serotonin and $0.51 \mu\text{A}$ for 17β -estradiol). Better results were obtained with nPEDOT; however, the increase in the current response was significantly higher with rGO/SPCE. This enhancement is attributed to the wrinkled surface of rGO, which increases the effective electrode area [34].

The electrochemical processes of serotonin and 17β -estradiol were investigated simultaneously by cyclic voltammetry (CV) using the $\text{Cu}(\text{L}^{\text{NO}_2})_2/\text{rGO}/\text{SPCE}$ in a potential range from 0.0 to 1.2 V and at a scan rate of 50 mV/s . As shown in Figure 6, two peaks were observed with modified $\text{Cu}(\text{L}^{\text{NO}_2})_2/\text{rGO}/\text{SPCE}$, indicating the simultaneous oxidation of serotonin and 17β -estradiol (Figure 6, red line). In contrast, the unmodified rGO/SPCE shows a peak corresponding to the serotonin and a very weak oxidation peak for 17β -estradiol (see inset of Figure 6). The signal enhancement observed when using $\text{Cu}(\text{L}^{\text{NO}_2})_2/\text{rGO}/\text{SPCE}$ can be ascribed to the synergistic effect between $\text{Cu}(\text{L}^{\text{NO}_2})_2$ and rGO which improves the electrocatalytic ability for the oxidation of 17β -estradiol. On the other hand, no reduction peak was observed for any of the analytes, indicating that the electrochemical process of serotonin and 17β -estradiol are irreversible. The oxidation peak of serotonin and 17β -estradiol was $+0.20$ and $+0.42 \text{ V}$ (vs. Ag/AgCl), respectively.

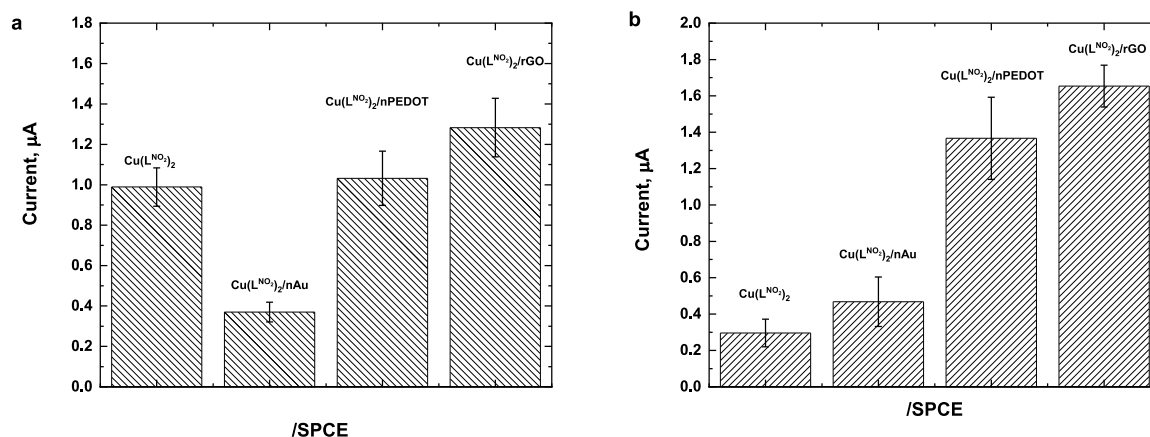


Figure 5. Electrochemical response of $25 \mu\text{mol L}^{-1}$ (a) serotonin and (b) 17β -estradiol obtained with different electrochemical platforms modified with 1 mg mL^{-1} of $\text{Cu}(\text{LNO}_2)_2$. Conditions: 40/60 EtOH/PB 0.1 mol L^{-1} , pH 7.0, $\text{Cu}(\text{LNO}_2)_2$ 1 mg/mL scan rate of 50 mV/s .

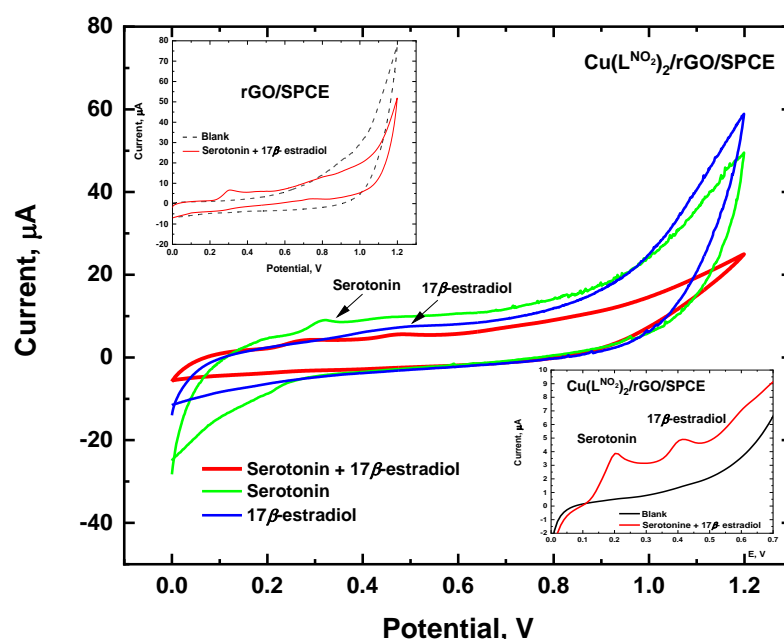


Figure 6. Electrochemical response simultaneous oxidation of $25 \mu\text{mol L}^{-1}$ serotonin and 17β -estradiol. Conditions: 40/60 EtOH/PB 0.1 mol L^{-1} , pH 7.0, $\text{Cu}(\text{LNO}_2)_2$ 1 mg/mL scan rate of 50 mV/s .

For a better understanding of the mechanism behind the electrochemical behavior of serotonin and 17β -estradiol on the $\text{Cu}(\text{LNO}_2)_2/\text{rGO}/\text{SPCE}$ and the possible role of atmospheric oxygen in the oxidation process, we carried out electrochemical measurement without oxygen, by continuous bubbling of N_2 into the solution, observing that the oxidation peaks of serotonin and 17β -estradiol remained unchanged at $+0.20$ and $+0.42 \text{ V}$ (vs. Ag/AgCl), respectively, which was indicative that the process electrochemical oxidation is independent of the presence of oxygen (see Figure S2 in supporting materials). The proposed mechanism for simultaneous serotonin and 17β -estradiol oxidation on the surface of $\text{Cu}(\text{LNO}_2)_2/\text{rGO}/\text{SPCE}$ is presented in Figure 7. According to the experimental results, the oxidation of serotonin is generated by a process via two electrons, similar to processes described for serotonin and dopamine [35–38], while the oxidation of 17β -estradiol corresponds to a process via one electron, similar to process previously described for 17β -estradiol [39–41], estriol [42], and bisphenol A [43].

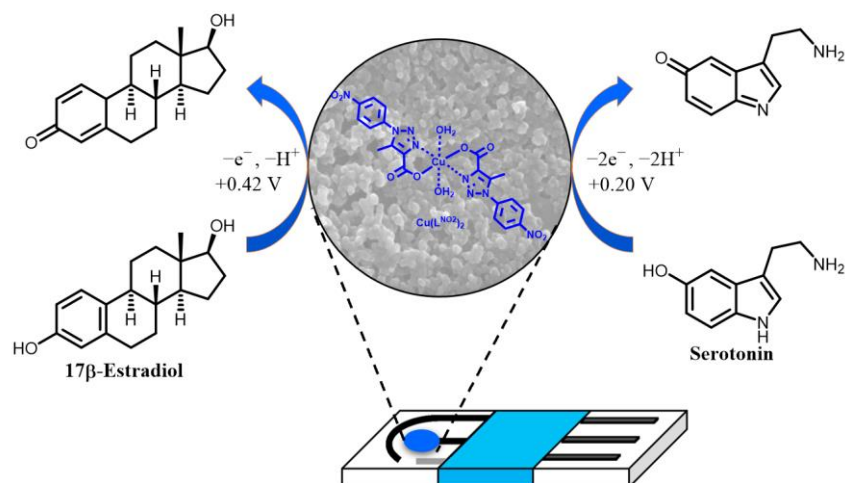


Figure 7. Proposed mechanism of serotonin and 17- β -estradiol oxidation at $\text{Cu}(\text{L}^{\text{NO}_2})_2/\text{rGO}/\text{SPCE}$.

3.4. Optimization of Parameters for LSV Serotonin and 17 β -Estradiol Simultaneous Detection

The effects of the concentration of $\text{Cu}(\text{L}^{\text{NO}_2})_2$ and pH of $\text{HPO}_4^{2-}/\text{PO}_4^{3-}$ solution on the oxidation current response of a mixture of serotonin and 17 β -estradiol were investigated using linear sweep voltammetry (LSV). As shown in Figure 8a, the serotonin oxidation peak current increased between pH 5.0 and pH 7.0, followed by a decrease at pH 8.0 and pH 10.0 which is attributable to the possible decomposition of the $\text{Cu}(\text{L}^{\text{NO}_2})_2$ complex as suggested by Nelson et al. [32]. Moreover, 17 β -estradiol maximal current response was observed at pH 6.0. On the other hand, for both analytes, a progressive shift of the E_p to less positive potentials were observed, indicating a pH-dependent behavior. The slope of the linear relationship between the E_p and pH for serotonin and 17 β -estradiol were -51 and -54 mV, respectively, close to the theoretical value of -59 mV. This confirms that an equal number of protons and electrons are involved in the electro-oxidation process of serotonin and 17 β -estradiol, as reported by Yu et. al. [34] and Brett et al. [44] (see Figure S3 in Supporting Materials). The concentration of $\text{Cu}(\text{L}^{\text{NO}_2})_2$ deposited over the electrode surface was evaluated in a range of 0.4 to 1.2 mg mL^{-1} (Figure 8b). The maximal current response for both analytes was obtained at complex concentration of 1.0 mg mL^{-1} . Adding higher concentrations of the complex led to a decrease in the signal current, which can be ascribed to the fact that at greater concentrations, 4-nitrophenyltriazole groups in the complex structure overlap each other, hindering electron transfer. Consequently, taking into account the equilibrium of the current response for serotonin and 17 β -estradiol, the optimum conditions selected for future studies were as follows: pH 7.0 for the $\text{HPO}_4^{2-}/\text{PO}_4^{3-}$ solution and a $\text{Cu}(\text{L}^{\text{NO}_2})_2$ concentration of 1.0 mg mL^{-1} .

3.5. Analytical Performance of $\text{Cu}(\text{L}^{\text{NO}_2})_2/\text{rGO}/\text{SPCE}$

Linear sweep voltammetry (LSV) was used for the simultaneous detection of serotonin and 17 β -estradiol under the optimum conditions previously described. Figure 9a shows the oxidation curves at $\text{Cu}(\text{L}^{\text{NO}_2})_2/\text{rGO}/\text{SPCE}$ and Figure 9b the linear relationships between the current response and concentrations for both analytes. The oxidation peak current for serotonin and 17 β -estradiol increases linearly with the concentration in a range of 2.0–42 $\mu\text{mol L}^{-1}$ ($R^2 = 0.9981$ for serotonin and $R^2 = 0.9978$ for 17 β -estradiol). For serotonin, the sensitivity was $0.064 \pm 0.001 \mu\text{A}/\mu\text{mol L}^{-1}$ and intercept was $0.069 \pm 0.02 \mu\text{A}/\mu\text{mol L}^{-1}$. For 17- β -estradiol, the sensitivity was $0.055 \pm 0.002 \mu\text{A}/\mu\text{mol L}^{-1}$ and the intercept was $-0.087 \pm 0.005 \mu\text{A}/\mu\text{mol L}^{-1}$. The LOD was calculated ($S/N = 3$) as described by Shrivastava et al. [45] for six measurements of blank. The values determined were 42 and 53 nmol L^{-1} for serotonin and 17 β -estradiol, respectively.

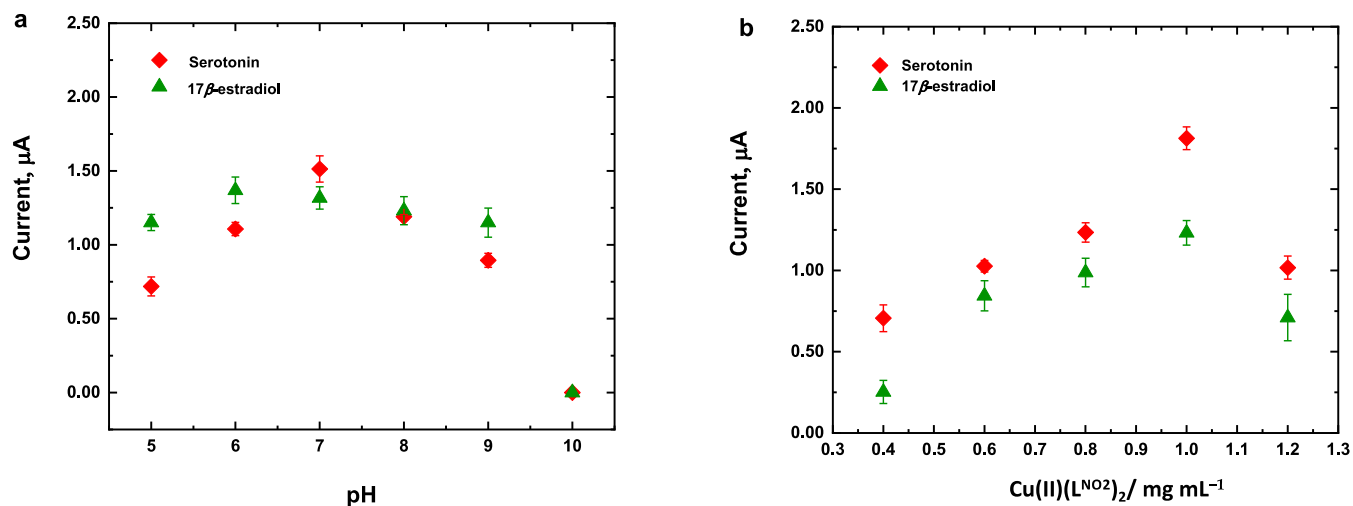


Figure 8. Optimization of experimental conditions of (a) pH and (b) Cu(LNO₂)₂ concentration for LSV electrochemical response of Cu(LNO₂)₂/rGO/SPCE for simultaneous analysis of 25 µmol L⁻¹ serotonin and 17β-estradiol.

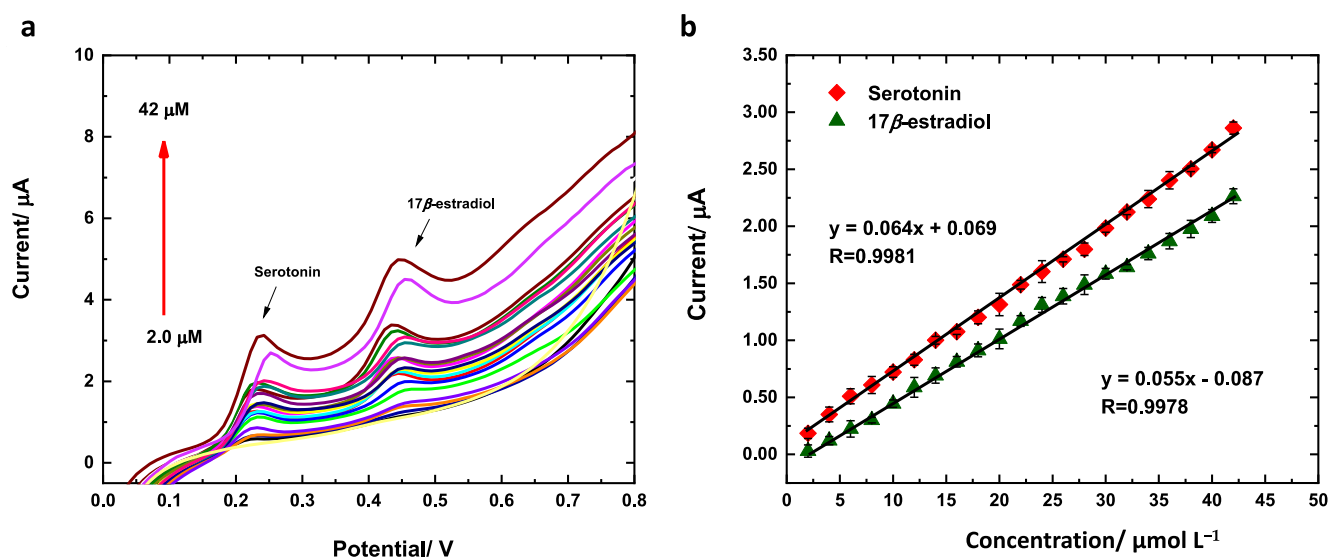


Figure 9. (a) Calibration curves and (b) LSV responses of Cu(LNO₂)₂/rGO/SPCE for the simultaneous analysis of 25 µmol L⁻¹ serotonin and 17β-estradiol. Conditions: 40/60 EtOH/PB 0.1 mol L⁻¹, pH 7.0, Cu(LNO₂)₂ 1 mg/mL and scan rate of 50 mV/s.

The methodology developed based on the preparation of Cu(LNO₂)₂/rGO/SPCE was compared with other electrochemical sensors previously reported since 2020 (Table 1). The LDs for the analytes, serotonin, and estradiol were considerably low. The use of the bidentate triazole complex combined with the characteristics of rGO increased the electrocatalytic capacity and allowed a speciation of these analytes through the difference in their oxidation potential.

Table 1. Comparison of the $\text{Cu}(\text{L}^{\text{NO}_2})_2/\text{rGO}/\text{SPCE}$ with other electrochemical sensor-modified electrodes for detecting serotonin and 17β -estradiol.

Analyte	Electrode	Lineal Range $\mu\text{mol L}^{-1}$	LOD nmol L^{-1}	Sample	Ref.
Serotonin	FeC-AuNPs-MWCNT/SPCE	0.05–20	17	urine	[46]
	DGNW/SPGE	1–500	280	urine	[47]
	TiO ₂ NP/AuNP/PNBDES/SPCE	0.3–20	2.47	human blood serum	[28]
	CDP-Choline/MCPE	10–30	3960	No reported human	[48]
	ZrO ₂ -CuO-CeO ₂ /Gr/CPE	7.9–205	3.49	urine/plasma samples	[29]
	ITO/CuO-Cu ₂ O	2–100	120	human blood serum	[49]
	p-AZ/MWCNT-GR/CFMEA	0.1–20	14.2	human serum	[50]
	$\text{Cu}(\text{L}^{\text{NO}_2})_2/\text{rGO}/\text{SPCE}$	2–42	42	human serum/Urine	This Work
17β -estradiol	α -Fe ₂ O ₃ -CNT/GCE	0.005–0.1	4.4	pharmaceutical/lake water/synthetic urine	[51]
	rGO-AuNPs/CNT/SPE	0.05–1.00	3	drinking water	[30]
	NiFe ₂ O ₄ -MC/GCE	0.02–0.566	6.88	estradiol in tablet	[52]
	wMC/GCE	0.05–10.0	8.3	Milk/real water	[31]
	CDs-PANI/GCE	0.001–100	43	human serum/different types of water	[35]
	CeO ₂ NPs/CPE	0.01–0.1	1.3/4.3	underground and lake water	[53]
	MIP-MWCNT/GCE	0.05–5.00	10	natural water samples	[54]
	$\text{Cu}(\text{L}^{\text{NO}_2})_2/\text{rGO}/\text{SPCE}$	2–42	53	human serum/Urine	This work

3.6. Repeatability, Stability, and Selectivity of the $\text{Cu}(\text{L}^{\text{NO}_2})_2/\text{rGO}/\text{SPCE}$

The repeatability of the analytical method was determined from the responses at 15 consecutive measurements in the presence of $25 \mu\text{mol L}^{-1}$ of a mixed solution of serotonin and 17β -estradiol. The relative standard deviations obtained were 10.6 and 9.1%, respectively. For stability studies, the electrode was stored at 4°C for 15 days and the measurements were made every day. Figure 10a,b shows that the fabricated sensor exhibited a relative standard deviation (RSD) for serotonin of 6.1% after 10 days and 15% after 15 days. The RSD for 17β estradiol is 14.6% after 10 days and 15% after 15 days, suggesting satisfactory storage stability. The effect of some electroactive substances with similar oxidation potential of serotonin and 17β -estradiol was investigated utilizing LVS in the potentials range of 0.0 to 1.2 V and at a scan rate of 50 mV/s in 40/60 EtOH/PB 0.1 mol L^{-1} , pH 7.0. Initially, $20 \mu\text{mol L}^{-1}$ of uric acid and ascorbic acid were studied, though no current signal was detected (see Figure S4 in supporting materials). Dopamine, which has a catechol group, was investigated at three concentration levels: 5, 10, and $20 \mu\text{mol L}^{-1}$. No current signal was detected at 5 and $10 \mu\text{mol L}^{-1}$; however, at $20 \mu\text{mol L}^{-1}$, a current signal was detected at 0.41 V (see Figure S5 in supporting materials). The effect of $20 \mu\text{mol L}^{-1}$ of dopamine on the oxidation peak of $20 \mu\text{mol L}^{-1}$ of serotonin and 17β -estradiol was investigated. The percentage values of current change in the presence of dopamine were 16.9% for serotonin and 6.1% for 17β -estradiol and the current signal peaks were shifted to more positive potentials, 0.31 V for serotonin and 0.52 V for 17β -estradiol (see Figure 10c). The similar oxidation potential of dopamine can be explained because the bidentate nature of catechols, such as dopamine, favors interactions with Cu(II) complexes, facilitating the oxidation of dopamine instead of serotonin and 17β -estradiol [55–57].

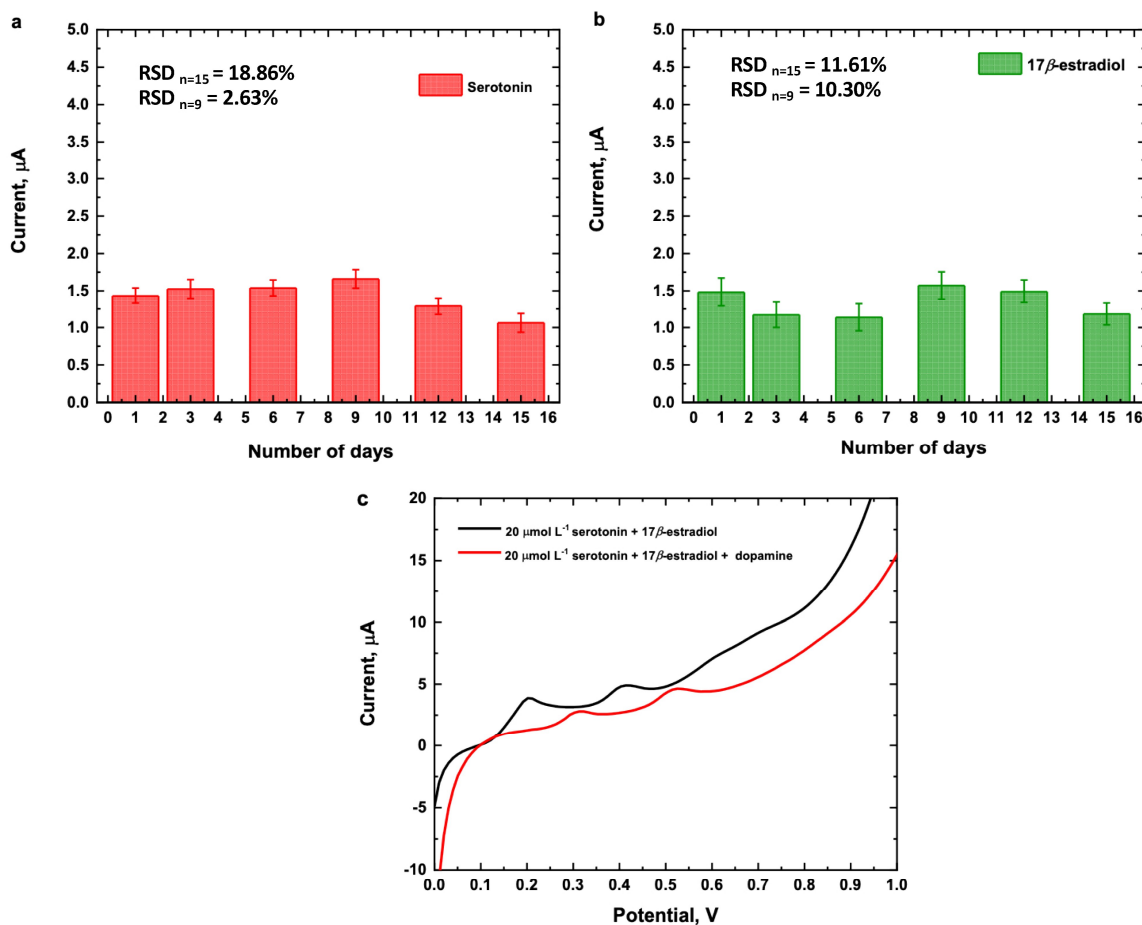


Figure 10. Current measurements of $25 \mu\text{mol L}^{-1}$ (a) serotonin, (b) 17β -estradiol and (c) $20 \mu\text{mol L}^{-1}$ of a mixture of serotonin and 17β -estradiol in presence of $20 \mu\text{mol L}^{-1}$ of dopamine. Conditions: 40/60 EtOH/PB 0.1 mol L^{-1} , pH 7.0, $\text{Cu}(\text{L}^{\text{NO}_2})_2$ 1 mg/mL and scan rate of 50 mV/s .

3.7. Evaluation of the Performance of $\text{Cu}(\text{L}^{\text{NO}_2})_2/\text{rGO}/\text{SPCE}$ for Detection Serotonin and 17β -Estradiol

In order to assess its applicability, the fabricated $\text{Cu}(\text{L}^{\text{NO}_2})_2/\text{rGO}/\text{SPCE}$ and the analytical method were evaluated for measuring the quantity of serotonin and 17β -estradiol in serum and synthetic human urine using the standard addition method. The pH of human serum was measured at 7.3 and that of synthetic human urine at 6.0. Due to the complexity of the matrices, the current of the oxidation signals exhibited a negative shift in both matrices, as illustrated in Figure 11a,b. According to the calibration curve obtained, the recovery concentration values of the spiked samples are shown in Table 2. These values ranged between 85 and 96%, with a RSD% of $\leq 7.0\%$, indicating that the electrode fulfills its intended purpose under the optimal parameters.

Table 2. Determination of serotonin and 17β -estradiol in synthetic serum and human urine samples using $\text{Cu}(\text{L}^{\text{NO}_2})_2/\text{rGO}/$.

Sample	Analyte	Added, mmol L^{-1}	Found mmol L^{-1}	Recovery, %	RSD, %
Human Serum *	Serotonin	0.15	0.134	89.3	2.8
	17β -estradiol	0.15	0.121	85.1	6.9
Human Urine †	Serotonin	0.15	0.145	96.7	1.9
	17β -estradiol	0.15	0.144	96.0	4.3

* Serotonin levels in human serum 0.28 and $1.14 \mu\text{mol L}^{-1}$; 17β -estradiol levels in human serum 0.11 to 1.5 nmol L^{-1} [58,59]. † Serotonin levels in human urine $> 2.5 \mu\text{mol L}^{-1}$ [46].

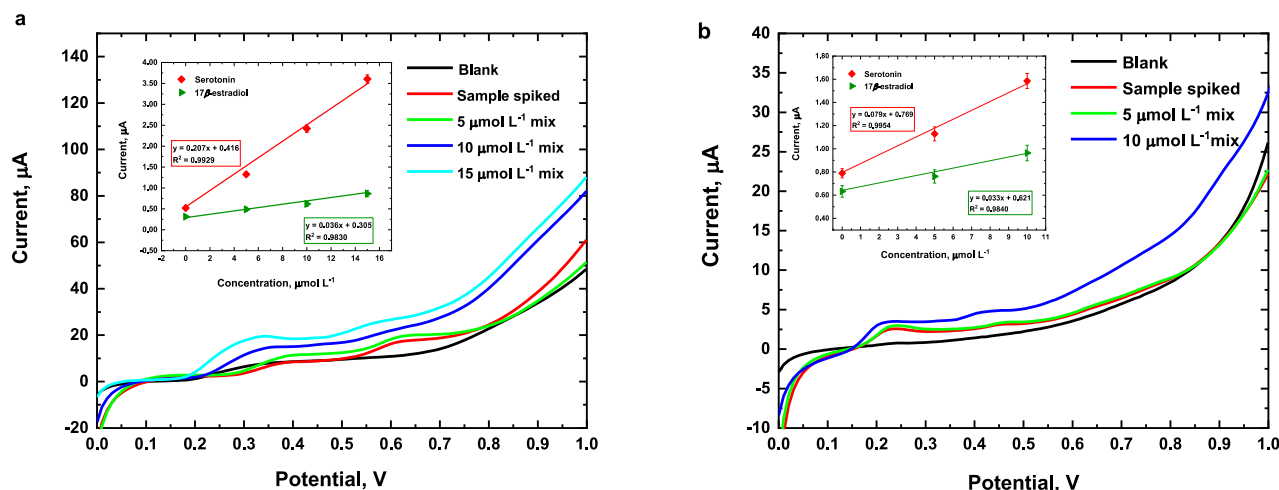


Figure 11. Electrochemical response of human serum (a) and synthetic human urine (b) spiked with different concentrations of a mixture of serotonin and 17 β -estradiol. Conditions: 40/60 EtOH/PB 0.1 mol L⁻¹, pH 7.0, Cu(L^{NO2})₂ 1 mg/mL, and scan rate of 50 mV/s.

4. Conclusions

As has been described, the rapid and direct effect of 17 β -estradiol on brain membranes is capable of modifying the availability of the serotonin receptor, which underscores its importance in the regulation of emotional disorders in women. However, to date, no research has been reported where methodologies are developed that allow the simultaneous determination of these analytes in diseases with a gender focus. In this work, it was possible to achieve significantly low detection limits for Cu(L^{NO2})₂/rGO/SPCE, considering levels reported in previous works (Table 1). It was also possible to simultaneously determine serotonin and 17 β -estradiol in enriched samples of human serum and urine with good accuracy and validity. Therefore, it can be concluded that the proposed method has a high potential for monitoring these analytes in samples of human biological fluids. Nevertheless, further research is required to achieve the quantification of 17 β -estradiol with the required accuracy. On the other hand, it is important to highlight that the development of these devices could bridge the gap between sophisticated analytical techniques and user demands for convenience, ease of operation, versatility, and prompt results, and contribute to improving the diagnosis and treatment of multisystemic diseases.

Supplementary Materials: The following supporting information can be downloaded at: <https://www.mdpi.com/article/10.3390/chemosensors12080164/s1>, Figure S1. EDS spectra of Cu(L^{NO2})₂/rGO/SPCE. Table S1. Equivalent circuit element values obtained by full nonlinear least squares fit of the EIS spectra. Figure S2. LSV electrochemical response of Cu(L^{NO2})₂/rGO/SPCE for simultaneous analysis. Figure S3. Effect of pH on the oxidation peak potential of 25 μ mol L⁻¹ of serotonin and 17 β -estradiol. Figure S4. LVS of 20 μ mol L⁻¹ of ascorbic and uric acid. Figure S5. LVS different concentrations of dopamine.

Author Contributions: C.N.: Writing—original draft, project administration, methodology, investigation, data curation, conceptualization, and supervision. R.N.: Investigation, formal analysis, review & editing, and supervision. G.T.: Investigation, formal analysis, review, and data curation. P.P.: Investigation, formal analysis, review, and data curation. R.C.: Investigation, formal analysis, review, and data curation. A.M.: Investigation, formal analysis, review & editing, and data curation. All authors have read and agreed to the published version of the manuscript.

Funding: This research was funded by ANID FONDECYT, Chile (Postdoctoral N°3210269) and 202211010037-VRIDT-UCN.

Institutional Review Board Statement: Not applicable.

Informed Consent Statement: Not applicable.

Data Availability Statement: The original contributions presented in the study are included in the article. Further inquiries can be directed to the corresponding author.

Acknowledgments: The authors would like to thank the Unidad de Equipamiento Científico MAINI-UCN for allowing us to use FE-SEM SU5000 and Confocal Raman Microscope.

Conflicts of Interest: The authors declare no conflicts of interest.

References

1. Halbreich, U.; Borenstein, J.; Pearlstein, T. The Prevalence, Impairment, Impact, and Burden of Premenstrual Dysphoric Disorder (PMS/PMDD). *Psychoneuroendocrinology* **2003**, *28*, 1–23. [\[CrossRef\]](#)
2. Hofmeister, S.; Bodden, S.; Colledge, M. Premenstrual Syndrome and Premenstrual Dysphoric Disorder. *Am. Fam. Physician* **2016**, *94*, 236–240.
3. Ducasse, D.; Jaussent, I.; Olié, E.; Guillaume, S. Personality Traits of Suicidality Are Associated with Premenstrual Syndrome and Premenstrual Dysphoric Disorder in a Suicidal Women Sample. *PLoS ONE* **2016**, *11*, e0148653. [\[CrossRef\]](#)
4. Slyepchenko, A.; Minuzzi, L.; Frey, B.N. Comorbid Premenstrual Dysphoric Disorder and Bipolar Disorder: A Review. *Front. Psychiatry* **2021**, *12*, 719241. [\[CrossRef\]](#)
5. American Psychiatric Association. *Diagnostic and Statistical Manual of Mental Disorders (DSM-5)*, 5th ed.; American Psychiatric Association: Washington, DC, USA, 2013.
6. Hantsoo, L.; Epperson, C.N. Premenstrual Dysphoric Disorder: Epidemiology and Treatment. *Curr. Psychiatry Rep.* **2015**, *28*, 87. [\[CrossRef\]](#) [\[PubMed\]](#)
7. Prasad, D.; Wollenhaupt-Aguiar, B.; Kidd, K.N.; Cardoso, T.D.A.; Frey, B.N. Suicidal Risk in Women with Premenstrual Syndrome and Premenstrual Dysphoric Disorder: A Systematic Review and Meta-Analysis. *J. Women's Health* **2021**, *30*, 1693–1707. [\[CrossRef\]](#)
8. Leenaars, A.A.; Dogra, T.D.; Girdhar, S.; Dattagupta, S.; Leenaars, L. Menstruation and suicide: A histopathological study. *Crisis* **2009**, *30*, 202–207. [\[CrossRef\]](#)
9. Papadopoulou, A.; Efstathiou, V.; Christodoulou, C.; Gournellis, R. Clinical and Psychometric Features of Psychiatric Patients after a Suicide Attempt in Relation with Menstrual Cycle Phases. *Arch. Women's Ment. Health* **2019**, *22*, 605–611. [\[CrossRef\]](#)
10. Yan, H.; Ding, Y.; Guo, W. Suicidality in Patients with Premenstrual Dysphoric Disorder—A Systematic Review and Meta-Analysis. *J. Affect. Disord.* **2021**, *295*, 339–346. [\[CrossRef\]](#)
11. Osborn, E.; Brooks, J.; Brien, P.M.S.O.; Wittkowski, A. Suicidality in Women with Premenstrual Dysphoric Disorder: A Systematic Literature Review. *Arch. Women's Ment. Health* **2021**, *24*, 173–184. [\[CrossRef\]](#)
12. Gao, M.; Qiao, M.; An, L.; Wang, G.; Wang, J.; Song, C.; Wei, F.; Yu, Y.; Gong, T.; Gao, D. Brain Reactivity to Emotional Stimuli in Women with Premenstrual Dysphoric Disorder and Related Personality Characteristics. *Aging* **2021**, *13*, 19529–19541. [\[CrossRef\]](#)
13. Critchley, H.O.; Babayev, E.; Bulun, S.E.; Clark, S.; Garcia-Grau, I.; Gregersen, P.K.; Kilcoyne, A.; Kim, J.-Y.; Lavender, M.; Marsh, E.E.; et al. Expert Reviews Menstruation: Science and Society. *Am. J. Obstet. Gynecol.* **2020**, *223*, 624–664. [\[CrossRef\]](#)
14. Nappi, R.E.; Cucinella, L.; Bosoni, D.; Righi, A.; Battista, F.; Molinaro, P.; Stincardini, G.; Piccinino, M.; Rossini, R.; Tiranini, L. Premenstrual Syndrome and Premenstrual Dysphoric Disorder as Centrally Based Disorders. *Endocrines* **2022**, *3*, 127–138. [\[CrossRef\]](#)
15. Nayman, S.; Beddig, T.; Reinhard, I.; Kuehner, C. Effects of Cognitive Emotion Regulation Strategies on Mood and Cortisol in Daily Life in Women with Premenstrual Dysphoric Disorder. *Psychol. Med.* **2023**, *53*, 5342–5352. [\[CrossRef\]](#) [\[PubMed\]](#)
16. Hantsoo, L.; Epperson, C.N. Allopregnanolone in Premenstrual Dysphoric Disorder (PMDD): Evidence for Dysregulated Sensitivity to GABA-A Receptor Modulating Neuroactive Steroids across the Menstrual Cycle. *Neurobiol. Stress* **2020**, *12*, 100213. [\[CrossRef\]](#)
17. Dubol, M.; Epperson, C.N.; Lanzenberger, R.; Sundström-poromaa, I. Neuroimaging Premenstrual Dysphoric Disorder: A Systematic and Critical Review. *Front. Neuroendocrinol.* **2020**, *57*, 100838. [\[CrossRef\]](#)
18. Alevizou, F.; Voursora, E.; Leonardou, A. Premenstrual Dysphoric Disorder: A Critical Review of Its Phenomenology, Etiology, Treatment and Clinical Status. *Curr. Women's Health Rev.* **2018**, *14*, 59–66. [\[CrossRef\]](#)
19. Andrzej, M.; Diana, J. Premenstrual Syndrome: From Etiology to Treatment. *Maturitas* **2006**, *55S*, S47–S54. [\[CrossRef\]](#)
20. Wu, Z.; Zhang, C.; Yang, C.; Zhang, X.; Wu, E. Simultaneous Quantitative Determination of Norgestrel and Progesterone in Human Serum by High-Performance Liquid Chromatography-Tandem Mass Spectrometry with Atmospheric Pressure Chemical Ionization. *Analyst* **2000**, *125*, 2201–2205. [\[CrossRef\]](#)
21. Pucci, V.; Bugamelli, F.; Mandrioli, R.; Luppi, B.; Raggi, M.A. Determination of Progesterone in Commercial Formulations and in Non Conventional Micellar Systems. *J. Pharm. Biomed. Anal.* **2003**, *30*, 1549–1559. [\[CrossRef\]](#)
22. Cao, W.; Gong, P.; Liu, W.; Zhuang, M.; Yang, J. A Sensitive Flow Injection Chemiluminescence Method for the Determination of Progesterone. *Drug Test. Anal.* **2013**, *5*, 242–246. [\[CrossRef\]](#)
23. Mishra, A.; Joy, K.P. HPLC-Electrochemical Detection of Ovarian Estradiol-17 β and Catecholestrogens in the catfish *Heteropneustes fossilis*: Seasonal and Perioviulatory Changes. *Gen. Comp. Endocrinol.* **2006**, *145*, 84–91. [\[CrossRef\]](#)
24. Sun, M.; Du, L.; Gao, S.; Bao, Y.; Wang, S. Determination of 17 β -Oestradiol by Fluorescence Immunoassay with Streptavidin-Conjugated Quantum Dots as Label. *Steroids* **2010**, *75*, 400–403. [\[CrossRef\]](#) [\[PubMed\]](#)

25. Ying, G.G.; Kookana, R.S.; Chen, Z. On-Line Solid-Phase Extraction and Fluorescence Detection of Selected Endocrine Disrupting Chemicals in Water by High-Performance Liquid Chromatography. *J. Environ. Sci. Health Part B* **2002**, *37*, 225–234. [[CrossRef](#)] [[PubMed](#)]
26. Ly, D.; Kang, K.; Choi, J.-Y.; Ishihara, A.; Back, K.; Lee, S.-G. HPLC Analysis of Serotonin, Tryptamine, Tyramine, and the Hydroxycinnamic Acid Amides of Serotonin and Tyramine in Food Vegetables. *J. Med. Food* **2008**, *11*, 385–389. [[CrossRef](#)] [[PubMed](#)]
27. Pussard, E.; Guigueno, N.; Adam, O.; Giudicelli, J.F. Validation of HPLC-Amperometric Detection to Measure Serotonin in Plasma, Platelets, Whole Blood, and Urine. *Clin. Chem.* **1996**, *42*, 1086–1091. [[CrossRef](#)] [[PubMed](#)]
28. Yılmaz, A.; Bilgi, M.; Yılmaz, M.; Atıcı, T. Ultra-Sensitive Electrochemical Sensors for Simultaneous Determination of Dopamine and Serotonin Based on Titanium Oxide-Gold Nanoparticles-Poly Nile Blue (in Deep Eutectic Solvent). *Electrochim. Acta* **2023**, *467*, 143046. [[CrossRef](#)]
29. Fazl, F.; Gholivand, M.B. High Performance Electrochemical Method for Simultaneous Determination Dopamine, Serotonin, and Tryptophan by ZrO₂-CuO Co-Doped CeO₂ Modified Carbon Paste Electrode. *Talanta* **2022**, *239*, 122982. [[CrossRef](#)] [[PubMed](#)]
30. Musa, A.M.; Kiely, J.; Luxton, R.; Honeychurch, K.C. Correction to: An Electrochemical Screen-Printed Sensor Based on Gold-Nanoparticle-Decorated Reduced Graphene Oxide-Carbon Nanotubes Composites for the Determination of 17-β Estradiol. *Biosensors* **2023**, *13*, 756. [[CrossRef](#)]
31. Xie, P.; Liu, Z.; Huang, S.; Chen, J.; Yan, Y.; Li, N.; Zhang, M.; Jin, M.; Shui, L. A Sensitive Electrochemical Sensor Based on Wrinkled Mesoporous Carbon Nanomaterials for Rapid and Reliable Assay of 17β-Estradiol. *Electrochim. Acta* **2022**, *408*, 139960. [[CrossRef](#)]
32. Cortés, P.; Castroagudín, M.; Kesternich, V.; Pérez-Fehrmann, M.; Carmona, E.; Zaragoza, G.; Vizcarra, A.; Hernández-Saravia, L.P.; Nelson, R. Ligand Influence in Electrocatalytic Properties of Cu(II) Triazole Complexes for Hydrogen Peroxide Detection in Aqueous Media. *Dalton Trans.* **2023**, *52*, 1476–1486. [[CrossRef](#)] [[PubMed](#)]
33. Hernández-Saravia, L.P.; Núñez, C.; Castroagudín, M.; Bertotti, M.; Vizcarra, A.; Arriaza, B.; Nelson, R. Development of a Fast and Simple Electrochemical Sensor for Trace Determination of Sulfite Using Copper(II) Triazole Complexes. *Microchem. J.* **2024**, *201*, 110560. [[CrossRef](#)]
34. Su, M.; Lan, H.; Tian, L.; Jiang, M.; Cao, X.; Zhu, C.; Yu, C. Ti₃C₂T_x-Reduced Graphene Oxide Nanocomposite-Based Electrochemical Sensor for Serotonin in Human Biofluids. *Sens. Actuators B Chem.* **2022**, *367*, 132019. [[CrossRef](#)]
35. Nehru, L.; Chinnathambi, S.; Fazio, E.; Neri, F.; Leonardi, S.G.; Bonavita, A.; Neri, G. Electrochemical Sensing of Serotonin by a Modified MnO₂-Graphene Electrode. *Biosensors* **2020**, *10*, 33. [[CrossRef](#)] [[PubMed](#)]
36. Dăscălescu, D.; Apetrei, C. Nanomaterials Based Electrochemical Sensors for Serotonin Detection: A Review. *Chemosensors* **2021**, *9*, 14. [[CrossRef](#)]
37. Baluta, S.; Zajac, D.; Szyszka, A.; Malecha, K.; Cabaj, J. Enzymatic Platforms for Sensitive Neurotransmitter Detection. *Sensors* **2020**, *20*, 423. [[CrossRef](#)] [[PubMed](#)]
38. Xu, Q.; Luo, L.; Liu, Z.; Guo, Z.; Huang, X. Highly Sensitive and Selective Serotonin (5-HT) Electrochemical Sensor Based on Ultrafine Fe₃O₄ Nanoparticles Anchored on Carbon Spheres. *Biosens. Bioelectron.* **2023**, *222*, 114990. [[CrossRef](#)] [[PubMed](#)]
39. Moraes, F.C.; Rossi, B.; Donatoni, M.C.; De Oliveira, K.T.; Pereira, E.C. Sensitive Determination of 17β-Estradiol in River Water Using a Graphene Based Electrochemical Sensor. *Anal. Chim. Acta* **2015**, *881*, 37–43. [[CrossRef](#)] [[PubMed](#)]
40. Supchocksoonthorn, P.; Alvirosinoy, M.C.; de Luna, M.D.G.; Paoprasert, P. Facile Fabrication of 17β-Estradiol Electrochemical Sensor Using Polyaniline/Carbon Dot-Coated Glassy Carbon Electrode with Synergistically Enhanced Electrochemical Stability. *Talanta* **2021**, *235*, 122782. [[CrossRef](#)] [[PubMed](#)]
41. Wang, Z.; Wang, P.; Tu, X.; Wu, Y.; Zhan, G.; Li, C. A Novel Electrochemical Sensor for Estradiol Based on Nanoporous Polymeric Film Bearing Poly{1-butyl-3-[3-(N-pyrrole)propyl]imidazole dodecyl sulfonate} Moiety. *Sens. Actuators B Chem.* **2014**, *193*, 190–197. [[CrossRef](#)]
42. Fu, H.; Wang, Y.; Dong, X.; Liu, Y.; Chen, Z.; Shen, Y.; Yang, C.; Dong, J.; Xu, Z. Application of Nickel Cobalt Oxide Nanoflakes for Electrochemical Sensing of Estriol in Milk. *RSC Adv.* **2016**, *6*, 65588–65593. [[CrossRef](#)]
43. Ananthakrishnan, D.; Venkatesvaran, H.; Kannan, A.; Gandhi, S. Simplistic One-Pot Synthesis of an Inorganic–Organic Cubic Caged Material: A New Interface for Detecting Toxic Bisphenol-A Electrochemically. *New J. Chem.* **2020**, *44*, 20192–20202. [[CrossRef](#)]
44. Masikini, M.; Ghica, E.; Baker, P.G.L.; Iwuoha, E.I.; Brett, C.M.A. Electrochemical Sensor Based on Multi-Walled Carbon Nanotube/Gold Nanoparticle Modified Glassy Carbon Electrode for Detection of Estradiol in Environmental Samples. *Electroanalysis* **2019**, *31*, 1925–1933. [[CrossRef](#)]
45. Shrivastava, A.; Gupta, V.B. Methods for the Determination of Limit of Detection and Limit of Quantitation of the Analytical Methods. *Chron. Young Sci.* **2011**, *2*, 21–25. [[CrossRef](#)]
46. Wu, B.; Yeasmin, S.; Liu, Y.; Cheng, L. Sensitive and Selective Electrochemical Sensor for Serotonin Detection Based on Ferrocene-Gold Nanoparticles Decorated Multiwall Carbon Nanotubes. *Sens. Actuator B Chem.* **2022**, *354*, 131216. [[CrossRef](#)]
47. Boonkaew, S.; Dettlaff, A.; Bogdanowicz, R.; Jönsson-niedzió, M. Electrochemical Determination of Neurotransmitter Serotonin Using Boron/Nitrogen Co-Doped Diamond-Graphene Nanowall-Structured Particles. *J. Electroanal. Chem.* **2022**, *926*, 116938. [[CrossRef](#)]

48. Deepa, S.; Kumara Swamy, B.E.; Vasantakumar Pai, K. Electrochemical Sensing Performance of Citicoline Sodium Modified Carbon Paste Electrode for Determination of Dopamine and Serotonin. *Mater. Sci. Energy Technol.* **2020**, *3*, 584–592. [[CrossRef](#)]
49. Salova, A.; Mahmud, S.F.; Almasoudie, N.K.A.; Mohammed, N.; Albeer, A.A.; Amer, R.F. CuO-Cu₂O Nanostructures as a Sensitive Sensing Platform for Electrochemical Sensing of Dopamine, Serotonin, Acetaminophen, and Caffeine Substances. *Inorg. Chem. Commun.* **2024**, *161*, 112065. [[CrossRef](#)]
50. Zeng, C.; Li, Y.; Zhu, M.; Du, Z.; Liang, H.; Chen, Q.; Ye, H.; Li, R.; Liu, W. Simultaneous Detection of Norepinephrine and 5-Hydroxytryptophan Using Poly-Alizarin/Multi-Walled Carbon Nanotubes-Graphene Modified Carbon Fiber Microelectrode Array Sensor. *Talanta* **2024**, *270*, 125565. [[CrossRef](#)] [[PubMed](#)]
51. Galvão, J.C.R.; Araujo, M.d.S.; Prete, M.C.; Neto, V.L.; Dall'Antonia, L.H.; Matos, R.; Tarley, C.R.T.; Medeiros, R.A. Electrochemical Determination of 17- β -Estradiol Using a Glassy Carbon Electrode Modified with α -Fe₂O₃ Nanoparticles Supported on Carbon Nanotubes. *Molecules* **2023**, *28*, 6372. [[CrossRef](#)] [[PubMed](#)]
52. Tanrikut, E.; Özcan, İ.; Sel, E.; Köytepe, S.; Savan, E.K. Simultaneous Electrochemical Detection of Estradiol and Testosterone Using Nickel Ferrite Oxide Doped Mesoporous Carbon Nanocomposite Modified Sensor. *J. Electrochem. Soc.* **2020**, *167*, 124107. [[CrossRef](#)]
53. Souza, M.B.; Santos, J.S.; Pontes, M.S.; Nunes, L.R.; Oliveira, I.P.; Lopez Ayme, A.J.; Santiago, E.F.; Grillo, R.; Fiorucci, A.R.; Arruda, G.J. CeO₂ Nanostructured Electrochemical Sensor for the Simultaneous Recognition of Diethylstilbestrol and 17 β -Estradiol Hormones. *Sci. Total Environ.* **2022**, *805*, 150348. [[CrossRef](#)]
54. Marques, G.L.; Rocha, L.R.; Prete, M.C.; Gorla, F.A.; Moscardi dos Santos, D.; Segatelli, M.G.; Teixeira Tarley, C.R. Development of Electrochemical Platform Based on Molecularly Imprinted Poly(Methacrylic Acid) Grafted on Iniferter-Modified Carbon Nanotubes for 17 β -Estradiol Determination in Water Samples. *Electroanalysis* **2021**, *33*, 568–578. [[CrossRef](#)]
55. Sandoval-Rojas, A.P.; Ibarra, L.; Cortés, M.T.; Macías, M.A.; Suescun, L.; Hurtado, J. Synthesis and Characterization of Copper(II) Complexes Containing Acetate and N,N-Donor Ligands, and Their Electrochemical Behavior in Dopamine Detection. *J. Electroanal. Chem.* **2017**, *805*, 60–67. [[CrossRef](#)]
56. Sanghavi, B.J.; Mobin, S.M.; Mathur, P.; Lahiri, G.K.; Srivastava, A.K. Biomimetic Sensor for Certain Catecholamines Employing Copper(II) Complex and Silver Nanoparticle Modified Glassy Carbon Paste Electrode. *Biosens. Bioelectron.* **2013**, *39*, 124–132. [[CrossRef](#)] [[PubMed](#)]
57. Boulkroune, M.; Chibani, A.; Geneste, F. Monocopper Complex Based on N-Tripodal Ligand Immobilized in a Nafion[®] Film for Biomimetic Detection of Catechols: Application to Dopamine. *Electrochim. Acta* **2016**, *221*, 80–85. [[CrossRef](#)]
58. Kikuchi, H.; Nakatani, Y.; Seki, Y.; Yu, X.; Sekiyama, T.; Sato-Suzuki, I.; Arita, H. Decreased Blood Serotonin in the Premenstrual Phase Enhances Negative Mood in Healthy Women. *J. Psychosom. Obstet. Gynecol.* **2010**, *31*, 83–89. [[CrossRef](#)] [[PubMed](#)]
59. Carretti, N.; Florio, P.; Bertolin, A.; Costa, C.V.L.; Allegri, G.; Zilli, G. Serum Fluctuations of Total and Free Tryptophan Levels during the Menstrual Cycle Are Related to Gonadotrophins and Reflect Brain Serotonin Utilization. *Hum. Reprod.* **2005**, *20*, 1548–1553. [[CrossRef](#)]

Disclaimer/Publisher's Note: The statements, opinions and data contained in all publications are solely those of the individual author(s) and contributor(s) and not of MDPI and/or the editor(s). MDPI and/or the editor(s) disclaim responsibility for any injury to people or property resulting from any ideas, methods, instructions or products referred to in the content.